Journal of Photochemistry and Photobiology A: Chemistry 312 (2015) 1–7

Contents lists available at ScienceDirect

Journal of Photochemistry and Photobiology A: Chemistry

journal homepage: www.elsevier.com/locate/jphotochem

Investigating the photo-oxidation of model indoor air pollutants using field asymmetric ion mobility spectrometry

Christopher P. Ireland*, Caterina Ducati

Department of Materials Science and Metallurgy, University of Cambridge, 27 Charles Babbage Road, Cambridge, CB3 0FS, United Kingdom

ARTICLE INFO

Article history:
Received 13 May 2015
Received in revised form 10 July 2015
Accepted 13 July 2015
Available online 20 July 2015

Keywords:
Photocatalysis
Indoor air purification
FAIMS
VOC degradation

ABSTRACT

We have developed a versatile measurement system utilising field asymmetric ion mobility spectrometry (FAIMS) to study the photocatalytic degradation of VOCs at concentrations comparable to indoor air. FAIMS allows continuous monitoring of chemical species in the gas phase, whilst having a high separation selectivity and sensitivity, so can be used to identify multiple species concurrently at ppb concentrations, which are clear advantages over traditional characterization techniques used in photocatalytic air purification such as gas chromatography. Here we demonstrate the methodology with the photo-oxidation of 2-propanol, ethanol and acetone using a commercial titanium dioxide felt. To the best of our knowledge, this is the first time FAIMS has been used in photocatalytic air purification applications.

1. Introduction

Since the early 1970s [1–2] there has been a steady increase in scientific research into photocatalysis, [3] centring on processes that can aid energy production such as water splitting, [4–5] or using photocatalysis for environmental clean up [6–7]. Whilst there are relatively few commercial applications of this technology, a focus in recent years has been using photocatalysis in indoor air purification, [8–9] with a significant number of patents filed in this area, [10] and commercial purification devices that use photocatalytic technology readily available. Indoor air quality is a problem that has come to the forefront recently, with the phenomenon of 'Sick Building Syndrome' being blamed for ill health in the workplace, leading to time off work, and lost production [11]. With volatile organic carbons (VOCs) present in indoor air, emanating from either the building itself through paint, sealant or wood stain, or from cleaning products such as deodorizers or floor cleaners, removal of these is a key priority, particularly as many VOCs are known to be mutagenic or carcinogenic [11]. Whilst air purification techniques such as filtration via activated carbon [12] or thermal advanced oxidation processes [13–14] can be effective, they have the disadvantage of requiring additional steps to process, in the case of activated carbon, or be carried out at high temperature and pressure, in the case of thermal advanced oxidation processes. Air purification using a photocatalyst has the advantage of operating at room temperature and pressure, with the final products of VOC purification being carbon dioxide and water. However, measuring accurately the low concentrations of VOC present in indoor air, typically in the ppb region, [11] can be challenging, and many photocatalysts can be tested for air purification properties at concentrations of VOC significantly higher than that of typical indoor air. This can be significant, as photo-oxidation is known to follow Langmuir–Hinshelwood kinetics, [15] which includes the concentration of molecule being photo-oxidised in the rate equation, so the effectiveness of photocatalysts at relatively high VOC concentrations is not a reliable indicator at their effectiveness at indoor air concentrations. Additionally, whilst monitoring the pollutants with gas chromatography or gas sensors, the products of photocatalytic air purification are not routinely investigated, and can require further characterisation techniques such as infra-red or mass-spectroscopy to monitor and identify intermediates; although carbon dioxide and water are known to be the final products, intermediates can be produced by the photocatalysis reaction, and these can be as harmful as the initial VOC being degraded. To this end, we have developed a versatile system for testing the effectiveness of catalysts for applications in indoor air purification using a field asymmetric ion mobility spectrometer (FAIMS) to monitor the air [16–18]. Unlike conventional techniques such as gas chromatography, or gas sensors designed for specific molecules, the FAIMS is capable of continuously detecting and monitoring concentrations of multiple air-born species in the ppb concentration range. Here we demonstrate this setup with the photocatalytic degradation of 2-propanol, ethanol and acetone on

* Corresponding author. Fax: + 44 1223 334567.
E-mail address: cpi20@cam.ac.uk (C.P. Ireland).

http://dx.doi.org/10.1016/j.jphotochem.2015.07.008

titanium dioxide irradiated with ultraviolet radiation. To the best of our knowledge, this is the first time that a FAIMS has been used in photocatalytic air purification applications, and is shown to be a simple and effective way of determining the photodegradation of typical indoor air pollutants.

2. Experimental

2.1. Materials

Model VOCs were obtained from evaporation of analytical reagent grade 2-propanol, ethanol, and acetone, purchased from Fisher Scientific UK. Saint-Gobain Quartz supplied the titanium dioxide based catalyst used in the experiments (Quartzel® PCO felt).

2.2. Permeation tubes

Permeation tubes were produced using a kit provided by Owlstone Ltd. A length of PTFE tubing, typically 14 cm, is sealed and crimped at one end. A small amount of VOC is poured into the PTFE tube, filling around half of the tube. The other end is then sealed and crimped. Under a continuous flow of air, the VOC permeates through the wall of the PTFE tubing at constant rate, due to the concentration gradient between the inner and outer tube surface. Once in the gas phase, the VOC is diluted into a carrier gas and can be extracted from the chamber. The diffusion rate, defined by Fick's law, can be determined gravimetrically. For further information, see reference [19].

2.3. Photocatalysis set up

For the photocatalysis experiments, a simple setup was developed (Fig. 1). A 2.5 L min^{-1} flow of medical grade compressed air was introduced into the dilution chamber enclosing the permeation tube(s) containing the required VOC. A constant flow of VOC diluted in air is carried though into a 250 ml reactor chamber, which is designed to contain the catalyst to be analysed. In all cases, the catalyst used was a strip of Quartzel® PCO felt, measuring 55 mm x 25 mm x 1 mm, weighing 0.03 g. The flow then enters the Owlstone Lonestar FAIMS, where the VOC is detected and its concentration is monitored. As the FAIMS is able to detect and identify any VOC with a high proton affinity, VOCs produced through the photocatalytic reaction can also be identified and measured continuously. The reactor chamber is positioned so that the centre is 15 cm from a UVitec UV lamp, consisting of 2×8 W tube lamps, with a peak photon emission wavelength of 365 nm, and an average intensity of 7 mW cm^{-1} (measured at the centre of the reactor using a photodiode). Unless otherwise stated, all experiments were carried out at low relative humidity, without any additional humidity added to the system.

2.4. Gas analysis

Gases are analysed by an Owlstone Lonestar FAIMS [20]. The analyser consists of a beta radiation source (Ni-63) emitting electrons that ionise the air and moisture that flows through the analyser at constant rate. This produces positive hydronium ions, $H^+(H_2O)_n$, as well as negative hydrated oxygen ions, $O^{2-}(H_2O)_n$. These positive and negative stable intermediate ions give rise to reactive ion peaks (RIP) in the positive and negative FAIMS spectra. If molecules with a high proton or electron affinity are present, such as VOCs including ethanol, acetone or 2-propanol, they can react with the intermediate ions, and replace one or two of the water molecules in the hydronium ion forming a positive monomer (M) or dimer (M_2) ion respectively (Eq. (1); VOCs could also react with the hydrated oxygen ion, forming a negative monomer or dimer ion (Eq. (3)) [20].

$$H^+(H_2O)_n + 2\,M + N_2 \leftrightarrow MH^+(H_2O)_n + M + N_2 + H_2O \leftrightarrow M_2H^+(H_2O)_n + N_2 + 2H_2O \quad (1)$$

$$O^{2-}(H_2O)_n + 2\,M + N_2 \leftrightarrow MO^{2-}(H_2O)_n + M + N_2 + H_2O \leftrightarrow M_2O^{2-}(H_2O)_n + N_2 + 2H_2O \quad (2)$$

The ions enter an electrode channel where, under an intense applied electric field and through collisions with the background gas, they reach a terminal velocity roughly proportional to the strength of the electric field [21]. An asymmetric radio frequency (RF) waveform is applied to create oscillating regions of high and low electric fields, which affect the ion's mobility, and hence their trajectories through the channel. The proportionality between ion mobility and electric field strength is compound dependant, which allows the separation of different ion species in the FAIMS [21]. A small compensation voltage is scanned between the top and bottom electrode, balancing the ion drift so that specific ions reach the detector rather than collide with the channel walls. The ion current that reaches the detector at a known compensation voltage is monitored and displayed by the FAIMS in the form of spectra, displaying compensation voltage vs. ion current, with the process taking only a few seconds. Increasing the applied peak-to-peak voltage of the RF waveform increases the field in the positive region, and decreases it in the negative region, which influences the velocity and so mobility of the ions; this has the effect of separating hydronium ions or hydrated oxygen ions from the monomer or dimer ions. By combining the ion current vs. compensation voltage plots acquired systematically from 0 to 100% of the maximum RF waveform, a matrix is produced which

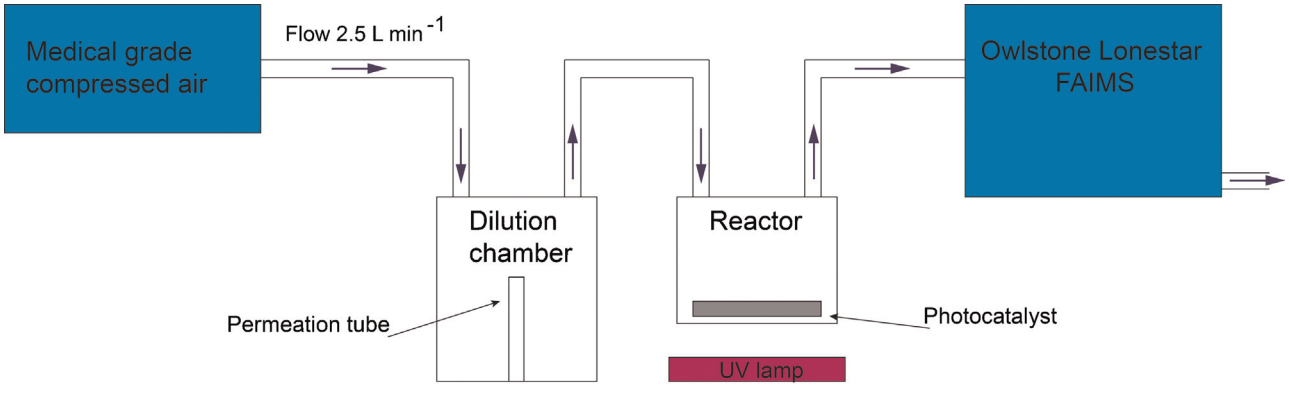

Fig. 1. Diagram illustrating the air photocatalysis setup developed for use with the Owlstone Lonestar FAIMS.

shows characteristic traces for reactive ion peaks (hydronium or hydrated oxygen ions), as well as product ion peaks, indicative of monomer or dimer ions formed from VOCs present in the sample [22]. The timing of this complete scan depends on the step change in the increase of the RF waveform; typically a high-resolution scan with a 2% step change can be carried out in 3 min. The systematic spectra show the ions separating as the RF waveform increases in intensity; by monitoring the spectra at a particular RF waveform strength where the ions are sufficiently separated to form two or more distinct peaks, whilst maintaining a high ion current, the height of these peaks is proportional to the concentration of ions entering the FAIMS. Whilst the ion peaks at specific %RF Values are centred at compensation voltage values, subtle changes in both flow and humidity can have an effect of shifting the peak positively or negatively, with the magnitude of these changes increasing with increasing DF; when monitoring peak height over time the peak height at a CV value +/− 0.1 V is recorded. Altering the flow can optimise the separation of peaks; decreasing the flow entering the FAIMS reduces the proportion of ions reaching the detector (transmission factor), but gives a smaller full width half maximum of the peaks, and so increases the resolution of the FAIMS. In our experiments, a flow rate of 2.5 L min^{-1} is ideal to allow a high transmission factor, with sensitively to separate the ion peaks being investigated. With the FAIMS continuously recording these spectra, this allows constant monitoring of monomer and dimer ions entering the FAIMS.

2.5. Electron microscopy

Electron microscopy imaging of the titanium dioxide based felt were carried out on a FEI Helios NanoLab FEG SEM/FIB microscope.

2.6. X-ray diffraction

X-ray diffraction (XRD) patterns for phase identification were collected using a Bruker D8 diffractometer using a copper X-ray source operating at 40 mA and 40 kV, fitted with a graphite second beam monochromator providing $K\alpha_1$ radiation at a wavelength of 1.5406 A. PXRD data were collected in $\theta/2\theta$ theta Bragg–Brentano geometry in the range 10–80 2θ with a step size of 0.02°, and a total data collection time of 1 h.

3. Results and discussion

3.1. Titanium dioxide based catalyst

For photocatalytic testing, a commercial titanium oxide based catalyst was chosen as a benchmark. The Quartzel® felt consists of silica fibres, coated with titanium dioxide by a sol–gel process [23]. XRD analysis shows broad peaks consistent with nano-size anatase TiO_2; there is no evidence of additional TiO_2 phases (Fig. 2a). SEM images (Fig. 2b) show there is a variation in thickness of the coated fibres in the range 8 μm–16 μm, and additional bulges with a diameter of 80 μm. The uncoated silica fibres have a reported diameter of 9 μm, indicating a titanium dioxide coating of up to a 4 μm layer on the fibres, with a thicker coating of TiO_2 accounting for the bulges. The surface area of the fibre is reported to be 120 $m^2 g^{-1}$ [23].

3.2. FAIMS analysis of model VOCs using permeation tubes

Ethanol was chosen for the initial testing of the system; a permeation tube containing ethanol was produced, and placed in the dilution chamber, with no catalyst present in the reactor. With a 2.5 L min^{-1} flow of medical grade compressed air flowing over the tube, ethanol emanating from the permeation tube is diluted and carried into the reactor and then into the FAIMS. After an initial stabilisation period, the FAIMS spectrum of ethanol can be recorded.

When the RF waveform of the FAIMS is at 60% of the maximum, the positive ion spectra of compensation voltage vs. ion current show a number of peaks (Fig. 3a). The peaks at –2.19 V and –1.70 V can be identified as hydronium ions (Eq. (1)); whilst one would normally expect a single peak for hydronium ions, the two peaks seen here could be the result of a fraction of the hydronium ions interacting with ion neutral ethanol, causing two peaks in the spectrum. The peak at –0.82 V corresponds to a hydronium ion that has reacted with ethanol forming a monomer ion (Eq. (1)); as the ion current is proportional to the concentration of ethanol [22], this ion current specifies the amount of ethanol entering the analyser after diffusing out of the permeation tube. Over the course of 3 days, the ion current at this peak remains constant; this confirms that ethanol continually permeates from the tube into the analyser (ESI, Fig. S1). From gravimetric measurements, the concentration of ethanol emanating from the permeation tube into the FAIMS can be estimated to be 70 ppb.

2-propanol can be monitored in a comparable manner. As 2-propnaol permeates from the permeation tube at a lower rate than ethanol due to the lower vapour pressure of 2-propanol, two permeation tubes containing 2-propanol were produced and placed in the dilution chamber, with the same 2.5 L min^{-1} flow of air allowing the diluted 2-propanol to enter the FAIMS. With the RF waveform again at 60%, a plot of compensation voltage vs. positive ion current shows the single peak of hydronium ions at −2.15 V, and 2-propanol monomer ions at −0.35 V, with the peak height proportional to the amount of 2-propanol that has entered the

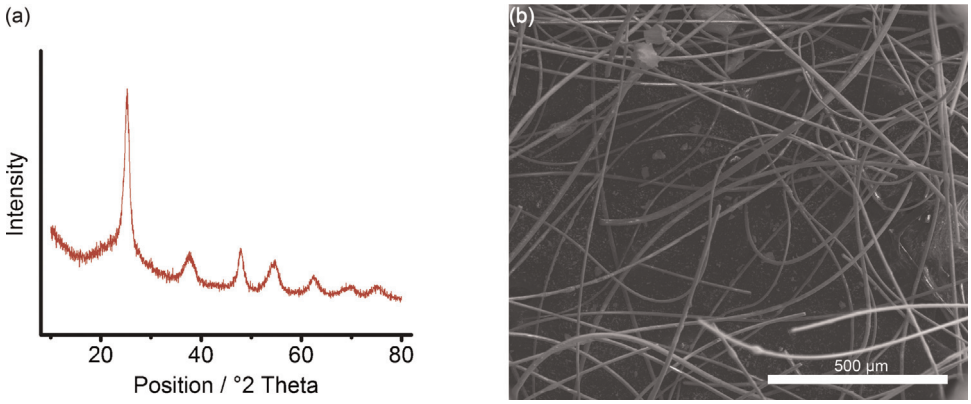

Fig. 2. (a) XRD spectra of the Quartzel® PCO felt. (b) SEM image of the Quartzel® PCO felt, at 100 × magnification.

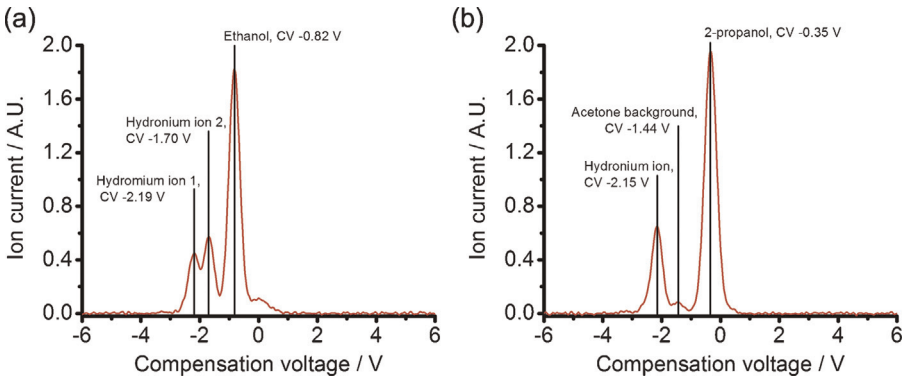

Fig. 3. (a) FAIMS Spectra obtained when ethanol is introduced to the analyser exclusively, and the RF waveform is set to 60% of maximum; peaks are assigned to hydronium ions, and ethanol monomer ions. (b) FAIMS Spectra obtained when 2-propanol is introduced to the analyser exclusively with the RF waveform set to 60% of maximum; peaks are assigned to hydronium ions, 2-propanol ions, with the small peak at −1.44 assigned tentatively to background acetone.

FAIMS (Fig. 3b). The small peak at −1.44 V, with an ion current of less than 0.1 V can be tentatively identified as background acetone; the low concentration makes identification difficult as the peak decreases into the background noise as the DF increases. As with ethanol, the ion current of the 2-propanol peak is constant over time, confirming 2-propanol continually permeates from the tubes (ESI, Fig. S2). From gravimetric measurements, the concentration of 2-propanol entering the FAIMS from both permeation tubes can be estimated to be 100 ppb.

These results confirm the stability of the permeation tubes as a source of low concentration VOCs; indeed the mechanism of VOC diffusing out of the permeation tube can be considered to be comparable to VOCs emanating from materials in the interior of buildings, and so photo degradation of this air would be an effective indicator of how well a photocatalyst will behave under interior air conditions. The monitoring of these VOCs highlights the advantage of this FAIMS analyser over a gas chromatograph for determining VOC concentration, in that it allows continuous monitoring as apposed to the batch sampling of gas chromatography.

A compensation voltage vs. ion current for acetone at 60% of the maximum waveform is shown in Fig. 4a. By systematically obtaining these compensation voltage vs. ion current plots from 0% to 100% of the maximum RF waveform of the FAIMS, then combining the spectra, 2D contour plots of ion current at a % of maximum RF waveform vs. compensation voltage were produced for acetone, as shown in Fig. 4b. (Comparable plots of ethanol and 2-propanol are in the supplementary information, ESI Fig. S3, Table S1, S2). These plots can be used as a specific 2D signature of each hydronium, monomer and dimer ions. Points along each of the branches in this plot can be referenced, stored, and used as a 'fingerprint' for the identification of unknown samples (ESI, Table S3). This technique can be expanded to a wide range of VOCs. This further highlights the effectiveness of FAIMS for use in this catalytic analysis, in that a range of VOCs can be effectively identified by this technique and the system can be "trained" to monitor different species [21–22]. Moreover, the continuous monitoring in addition to identification allows the monitoring of multiple species, which is another advantage over gas sensors, which are designed to determine concentrations for specific gases.

3.3. Photocatalytic air purification

A strip of Quartzel® felt, was placed in the reactor chamber in the dark, and two 2-propanol permeation tubes were placed in the dilution chamber. A 2.5 L min^{-1} flow of medical grade air was introduced through the setup, diluting and allowing 2-propanol to enter the reactor with the felt, then into the FAIMS. The amount of 2-propanol entering the FAIMS can be determined from the FAIMS spectrum of compensation voltage vs. ion current, monitoring the 2-propanol peak identified previously at CV -0.35 V, when the RF waveform is set to 60% maximum. With the felt present in the second chamber, the amount of 2-propanol being recorded is significantly less than previously recorded without the felt (Fig. 5a). As the airflow rate of 2.5 L min^{-1} is the same, and the two permeation tubes are continually diffusing 2-propanol, this

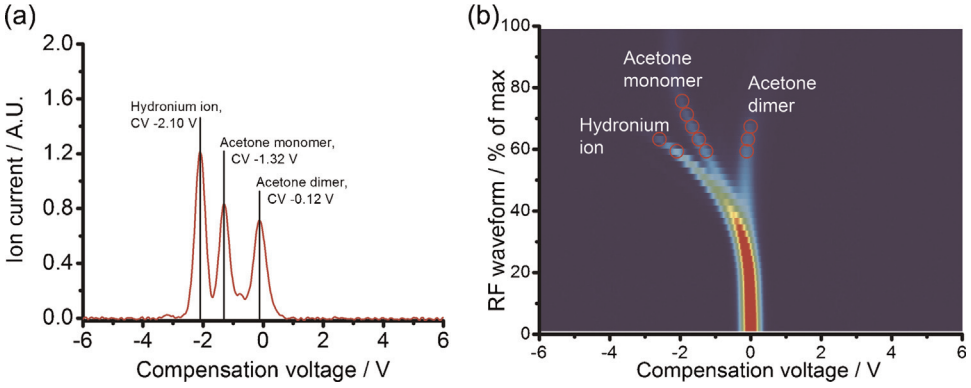

Fig. 4. (a) Spectra produced by the FAIMS when the RF waveform is 60% of maximum, and acetone is introduced to the analyser exclusively. (b) Contour plots showing the combined compensation voltage vs ion current plots as a function of varying the RF waveform from 0–100% of maximum, with the ion current represented low to high, by blue to red respectively on the map, when acetone is introduced exclusively into the analyser, with the points along the hydronium ion, acetone monomer and acetone dimer highlighted that are used to determine the identification of acetone in a FAIMS spectra.

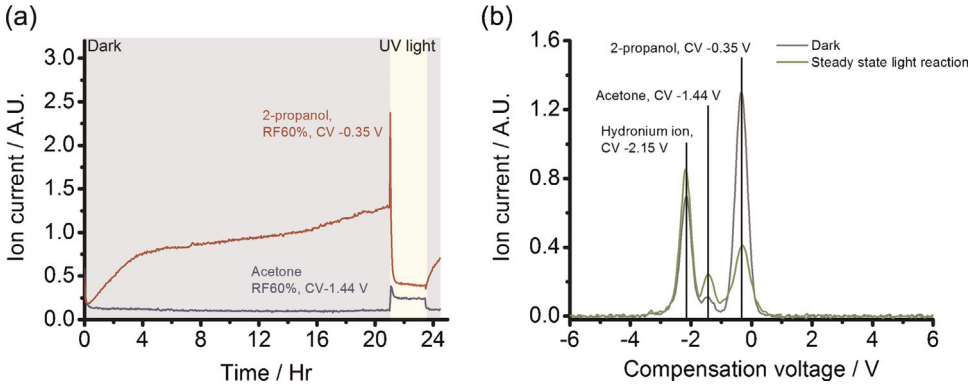

Fig. 5. (a) Graph showing the ion current at peaks from the compensation voltage vs ion current spectra produced during the 2-propanol photo-oxidation reaction when the RF waveform is at 60% of maximum; 2-propanol (red line) and acetone (blue line) shown, with the illuminated reaction highlighted. (b) Typical spectra produced by the FAIMS when the RF waveform is 60% of maximum when then reactor containing the felt is in the dark (grey line), and when it is illuminated (green line).

decrease in concentration of 2-propanol entering the FAIMS must be due to the VOC being adsorbed onto the surface of the catalyst. This process continued overnight; 2-propanol continually flowing through the reactor from the permeation tube. As time progressed, the concentration of 2-propanol that reached the FAIMS increased, suggesting that as the surface of the felt was being covered with 2-propanol, the adsorption onto the felt surface was decreasing. Just before illumination, the 2-propanol ion current in the presence of the felt (in the dark) had reached half that measured for the empty reactor.

When the UV light was turned on, there was an immediate increase in 2-propanol reaching the detector. As the rate of 2-propanol entering the reactor chamber remains constant, this increase must be due to an amount of 2-propanol becoming desorbed from the catalyst upon activation with UV light (Fig. 5a). At the same time, a stronger signal can be seen in the spectrum produced by the FAIMS at 60% of the maximum RF waveform when the when the felt is illuminated at −1.44 V. (Fig. 5a), compared to the spectrum produced just before illumination. An analysis of the 2d contour spectrum of compensation voltage vs. RF waveform produced when the felt is illuminated confirms that this additional signal is consistent with the presence of acetone; points along this additional signal can be matched with that of the acetone monomer measured previously (ESI, Figure S4). The acetone dimer ion seen in Fig. 5b is masked in this case by the 2-propanol. As illumination time continues, the amount of 2-propanol decreases significantly below the starting point, and remains at a steady-state constant level whilst the reactor is illuminated, with 2-propanol continually flowing into the reactor at an estimated concentration of 100 ppb (Fig. 5b). This implies that adsorbed 2-propanol on the surface is being photo-oxidised either into acetone, or directly into carbon dioxide and water. These products then desorb from the surface of the felt, and continue into the FAIMS, where the acetone is recorded at a steady concentration. Upon illumination, the hydronium ion current also increases. The primary reason for this is that there is a lower concentration of VOCs entering the FAIMS, hence more hydronium ions remain unreacted with VOCs to produce monomer or dimer ions; this further confirms some of the 2-propanol is converted to carbon dioxide and water. The higher hydronium ion concentration could also be due to this increase in water coming from the products of the photo-oxidation, although this cannot be confirmed due to the larger increase that results from the lower amount of VOCs present. With active sites free, further 2-propanol can now be adsorbed onto the surface; this limits the amount of 2-propanol reaching the FAIMS, accounting for the decrease in 2-propanol to approximately 25% of the 2-propanol emanating at the start of the reaction. These catalytic reaction steps of adsorption, reaction and desorption are continuous. The reaction was repeated with the same catalyst, and comparable photo-oxidation of 2-propanol was observed (ESI, Fig. S5).

The photo-oxidation of 2-propanol is well known, [24–25] with acetone as the product, and it is thought that whilst the photo-oxidation of 2-propanol to acetone is a fast reaction, the photo-oxidation of acetone to carbon dioxide and water or alternative products is slow. As the kinetics of photo-oxidation follows Langmuir–Hinshelwood kinetics, [15] the rate equation is partly determined by the adsorption of the molecule being oxidised onto the surface of the catalyst – the adsorption constant (Eq. (3)).

$$r = k'\theta_A = \frac{k'K_AC_A}{1 + K_AC_A} \quad (3)$$

A simplified Langmuir–Hinshelwood rate form of the rate equation for a typical gaseous photocatalytic reaction, with k' a pseudo-true rate constant, K_A the adsorption constant and C_A the concentration [15].

The results demonstrate that for acetone in this reaction, the adsorption coefficient is significantly less than that for 2-propanol, as can be seen by the decrease in concentration of 2-propanol reaching the FAIMS by nearly 75% from just before illumination, and by acetone desorbing and entering the FAIMS before photo-oxidation to carbon dioxide and water, indicating acetone is adsorbed less effectively than 2-propanol. The greater amount of acetone entering the analyser when the catalyst is initially illuminated further confirms the Langmuir–Hinshelwood kinetics. 2-propanol has been adsorbed previously in the dark, and this is immediately converted into acetone at a higher rate than the steady-state rate that the reaction reaches after this initial period when the system is illuminated. As the 2-propanol is already adsorbed onto the surface, it is immediately converted to acetone upon illumination, with the higher rate indicative of the 2-propanol adsorption coefficient not being involved in this initial rate. However as the adsorption coefficient of acetone is less than that for 2-propanol, much of the acetone desorbs and enters the FAIMS, resulting in the initial increase in the acetone amount entering the FAIMS. When the illumination ceases, the concentration of 2-propanol entering the FAIMS increases, indicating that the photo-oxidation has terminated; this is further confirmed by the amount of acetone entering the reactor decreasing to pre illumination levels.

The relative humidity of air is know to affect the photo-oxidation of 2-propanol, with higher relative humidity generally resulting in lower efficiencies, due to the competitive adsorption between water molecules and 2-propanol on the surface of the

catalyst [26]. Whilst the FAIMS works well at low relative humidity, the FAIMS can be operated at up to 95% humidity [20]. Increasing the humidity increases the ion current emanating from the hydronium ions, and the 2-propanol ion current is weaker; the more intense hydronium ion signals overlap the acetone signal, however a clear acetone peak can be seen at higher RF, and so can be used to monitor the acetone concentration during reactions. Again, two 2-propanol permeation tubes were introduced into the dilution chamber, and carried through to the reaction chamber containing a strip of Quartzel® felt, with the addition of a water beaker increasing the relative humidity of the reaction chamber, and left overnight. Upon illumination, initially a comparable reaction profile to that carried out at low relative humidity takes place, with an increase in 2-propanol entering the FAIMS due to 2-propanol desorbing from the surface, with a simultaneous increase in acetone. As the reaction proceeds, the 2-propanol concentration decreases, but not as significantly as under low relative humidity conditions, consistent with the observation the efficiency of the reaction decreases with increasing humidity. As observed previously, there is an increase in hydronium ion concentration, which is consistent with a lower overall amount of VOC entering the FAIMS. Acetone is also continually detected, confirming 2-propnaol is being photo-oxidised; after illumination terminates, the acetone concentration decreases (ESI, Fig. S6, S7).

The limited ability of the catalyst to degrade acetone can be corroborated by introducing acetone exclusively into the reaction chamber containing a strip of the Quartzel® felt by placing a permeation tube of acetone into the dilution chamber (Fig. 6a). It can be seen that the felt is only able to degrade around 30% of the acetone entering the reaction chamber when the reaction is at a steady state. This performance of the catalyst compared to the degradation of 2-propanol confirms the slow photo-oxidation of acetone. However, the steady-state level of acetone reaching the gas analyser whilst the system is illuminated, despite acetone continually permeating into the system, confirms the catalyst is degrading acetone, with the FAIMS detecting no further products, indicating the acetone has been converted into carbon dioxide and water. As with 2-propanol, when the UV lamp is turned off, there is an increase in acetone reaching the FAIMS.

The versatility of the measurement system can be demonstrated by the degradation of other VOCs such as ethanol using a comparable setup. By simply changing the permeation tube to ethanol, the photodegradation of the VOC can be monitored and quantified. Ethanol was introduced into the dilution chamber from a permeation tube, and carried into the reactor containing a strip of the Quartzel® felt, and left overnight. Upon illumination the concentration of ethanol, as monitored by the CV −0.82 V peak in the FAIMS spectra at an RF waveform of 60%, increases then decreases, following a comparable reaction path to 2-propanol, reaching a steady-state concentration after the initial increase (Fig. 6b). As with acetone, no VOC products were detected by the FAIMS, implying the ethanol has degraded directly into carbon dioxide and water. After illumination terminates, the amount of ethanol reaching the reactor increases, signifying the photo-oxidation has ceased.

This continuous monitoring of both reactants and products at concentrations comparable to indoor air VOC pollutants, highlight the effectiveness of this approach in determining the photocatalytic properties of materials that can be used for indoor air purification. GC/MS can be used to monitor this type of photocatalytic reaction [26–27], with mass-spectrometry capable of identifying intermediate species; infrared analysis of adsorbed species on the catalyst can also effectively identify possible intermediate species and products [28]. However FAIMS offers an effective alternative, where the monitoring of pollutants, intermediates and products takes place concurrently. With the 2-propanol reaction, intermediates such as acetone were monitored continuously during the reaction, in addition to the pollutant being degraded. The identification of the intermediates was carried out by comparing the additional signals produced during the reaction with that of known VOCs previously tested by the FAIMS. The ion current of the signal produced can be used to determine the concentration of intermediate with suitable calibration curves determined gravimetrically from permeation tubes of the intermediate. Whilst mass spectrometry offers the ability to identify unknown intermediates directly from the molecular weight peaks, the identity of many of these intermediates can be predicted by considering possible oxidation or reduction products of the initial contaminant; here, as in the case with acetone, FAIMS can be used to confirm the identity of these intermediates. The continuous nature of the FAIMS analysis can allow effective kinetic studies to be carried out on intermediates or products, which can be lacking in the batch process allowed in mass spectrometry, or particularly infrared studies of gas adsorbed onto the surface of the catalyst. Whilst not suggesting the FAIMS system is superior to GC/MS systems, which have been shown to be an effective instrument for investigating photocatalytic reactions, the continuous method and simplicity of the FAIMS presented here offers a flexible alterative, which has the potential to be a potent tool in indoor air purification studies.

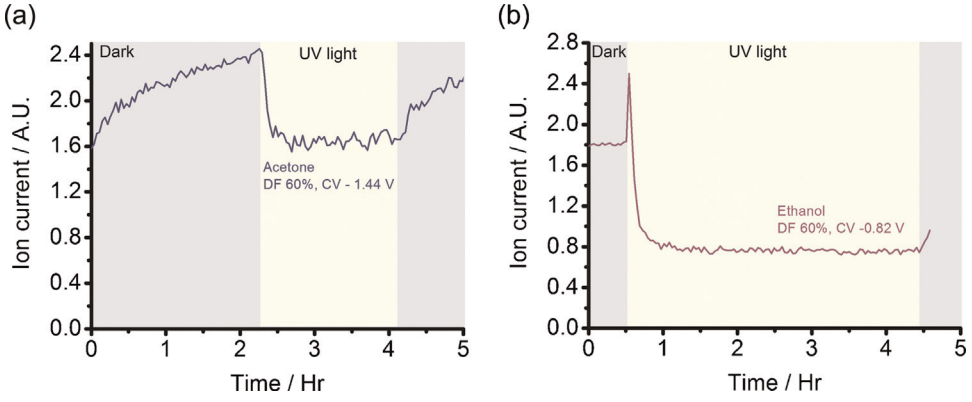

Fig. 6. (a) The positive ion current of acetone monomer ions entering the FAIMS, determined by the peak maximum at a compensation voltage of −1.44 V, when the RF waveform is at 60% of the maximum, with illumination time highlighted. (b) The positive ion current of ethanol monomer ions entering the FAIMS, determined by the peak maximum at a compensation voltage of −0.82 V, when the RF waveform is at 60% of the maximum, with illumination time highlighted.

4. Conclusion

We have developed a versatile measurement system for testing the effectiveness of photocatalysts at degrading volatile organic carbons at low concentrations comparable to those found in indoor air. Demonstrating this with the model VOC 2-propanol, we have used FAIMS technology to continually monitor 2-propanol during the course of the reaction, and follow the evolution of the product of the photo-oxidation, i.e. acetone. We have demonstrated the versatility of this system by additionally investigating the photo-oxidation of acetone and ethanol. To the best of our knowledge, this is the first time field asymmetric ion mobility spectrometry has been utilised in this way. FAIMS offers a significant advantage over previous systems that utilise gas chromatography, by allowing continuous monitoring of VOCs at ppb concentration levels. The simple setup will allow further photocatalysts and VOCs to be tested under comparable conditions, to further elucidate photo-catalytic gas reactions at low concentrations.

Acknowledgments

The authors are grateful for the financial support from the ERC, under grant number 259619 PHOTO EM and grant number 620298 PHOTO AIR (Proof of Concept); the authors wish to thank Russell Paris from Owlstone Ltd. for helpful discussions, Emma Copham for SEM images and Mike Coto for XRD.

Appendix A. Supplementary data

Data files related to this publication are available at the University of Cambridge data repository (https://www.repository.cam.ac.uk/handle/1810/248897).

Supplementary data associated with this article can be found, in the online version, at http://dx.doi.org/10.1016/j.jphotochem.2015.07.008.

References

[1] A. Fujishima, K. Honda, Bull. Chem. Soc. Jpn. 44 (1971) 1148–1150.
[2] A. Fujishima, K. Honda, Nature 238 (1972) 37–38.
[3] A. Mills, S. LeHunte, J. Photochem. Photobiol. A 108 (1997) 1–35.
[4] F.E. Osterloh, Chem. Mater. 20 (2008) 35–54.
[5] F.E. Osterloh, Chem. Mater. 42 (2013) 2294–2320.
[6] M.R. Hoffmann, S.T. Martin, W.Y. Choi, D.W. Bahnemann, Chem. Rev. 95 (1995) 69–96.
[7] H.J. Zhang, G.H. Chen, D.W. Bahnemann, J. Mater. Chem. 19 (2009) 5089–5121.
[8] J. Zhao, X.D. Yang, Build. Environ. 38 (2003) 645–654.
[9] J.H. Mo, Y.P. Zhang, Q.J. Xu, J.J. Lamson, R.Y. Zhao, Atmos. Environ. 43 (2009) 2229–2246.
[10] Y. Paz, Appl Catal. B 99 (2010) 448–460.
[11] S.B. Wang, H.M. Ang, M.O. Tade, Environ. Int. 33 (2007) 694–705.
[12] S. Sircar, T.C. Golden, M.B. Rao, Carbon 34 (1996) 1–12.
[13] H. Drysys, Filtr. Sep. 34 (1997) 324–329.
[14] K. Everaert, J. Baeyens, J. Hazard. Mater. 109 (2004) 113–139.
[15] J.M. Herrmann, Appl Catal. B 99 (2010) 461–468.
[16] R. Guevremont, J. Chromatogr. A 1058 (2004) 3–19.
[17] B.M. Kolakowski, Z. Mester, Analyst 132 (2007) 842–864.
[18] A.B. Kanu, P. Dwivedi, M. Tam, L. Matz, H.H. Hill, J, *Mass Spectrom.* 43 (2008) 1–22.
[19] Permeation Tubes and Diffusion Tubes. http://www.owlstonenanotech.com/calibration-gas-generator/permeation-tubes-and-diffusion-tubes (accessed April 2015).
[20] [20] Field Asymmetric Ion Mobility Spectrometry (FAIMS). http://www.owlstonenanotech.com/faims (accessed April 2015).
[21] R. Guevremont, R.W. Purves, Rev Sci. Instrum. 70 (1999) 1370–1383.
[22] R.A. Miller, G.A. Eiceman, E.G. Nazarov, A.T. King, Sens. Actuators. B 67 (2000) 300–306.
[23] H. Destaillats, M. Sleiman, D.P. Sullivan, C. Jacquiod, J. Sablayrolles, L. Molins, Appl. Catal. B 128 (2012) 159–170.
[24] R.I. Bickley, G. Munuera, F.S. Stone, J. Catal. 31 (1973) 398–407.
[25] S.A. Larson, J.A. Widegren, J.L. Falconer, J. Catal. 157 (1995) 611–625.
[26] D. Vildozo, C. Ferronato, M. Sleiman, J.M. Chovelon, Appl. Catal. B 94 (2010) 303–310.
[27] D. Vildozo, R. Portela, C. Ferronato, J.M. Chovelon, 107 (2011) 347–354.
[28] F. Bosc, D. Edwards, N. Keller, V. Keller, A. Ayral, Thin Solid Films 495 (2006) 272–279.